Neurochemical Research (2019) 44:2733–2745
https://doi.org/10.1007/s11064-019-02892-4

ORIGINAL PAPER

The Potassium Channel Kv1.5 Expression Alters During Experimental Autoimmune Encephalomyelitis

I. Bozic[1] · D. Savic[1] · A. Milosevic[1] · M. Janjic[1] · D. Laketa[2] · K. Tesovic[1] · I. Bjelobaba[1] · M. Jakovljevic[1] · N. Nedeljkovic[2] · S. Pekovic[1] · I. Lavrnja[1]

Received: 23 July 2019 / Revised: 23 September 2019 / Accepted: 11 October 2019 / Published online: 17 October 2019

Abstract

Multiple sclerosis (MS) is a chronic, inflammatory, neurodegenerative disease with an autoimmune component. It was suggested that potassium channels, which are involved in crucial biological functions may have a role in different diseases, including MS and its animal model, experimental autoimmune encephalomyelitis (EAE). It was shown that voltage-gated potassium channels Kv1.5 are responsible for fine-tuning in the immune physiology and influence proliferation and differentiation in microglia and astrocytes. Here, we explored the cellular distribution of the Kv1.5 channel, together with its transcript and protein expression in the male rat spinal cord during different stages of EAE. Our results reveal a decrease of Kv1.5 transcript and protein level at the peak of disease, where massive infiltration of myeloid cells occurs, together with reactive astrogliosis and demyelination. Also, we revealed that the presence of this channel is not found in infiltrating macrophages/microglia during EAE. It is interesting to note that Kv1.5 channel is expressed only in resting microglia in the naïve animals. Predominant expression of Kv1.5 channel was found in the astrocytes in all experimental groups, while some vimentin$^+$ cells, resembling macrophages, are devoid of Kv1.5 expression. Our results point to the possible link between Kv1.5 channel and the pathophysiological processes in EAE.

Keywords MS · EAE · Potassium channels · Kv1.5 · Astrocytes

Introduction

Multiple sclerosis (MS) is a chronic, immune-mediated disease, characterized by prominent demyelination and neurodegeneration. In human patients and animal model of the disease, experimental autoimmune encephalomyelitis (EAE), the pathology is initiated by primed immune cells, mainly T cells, B cells, and macrophages, which cross the blood–brain (BBB) and blood-cerebrospinal fluid barriers and enter into the central nervous system (CNS) parenchyma. The ensuing interplay between the peripheral and innate immune cells of the CNS, microglia, and astrocytes, leads to neuroinflammation which drives further pathology. Activation of the glial cells is crucial for the development of the disease, which culminates in the myelin sheet and axonal loss [1].

Neuronal cell homeostasis crucially depends on the proper functioning of ion channels, which mediate facilitated diffusion of mobile ions across the cell membrane [2]. Among them, potassium channels play significant roles in neuronal homeostasis, as they contribute to both the resting and excited state of the cells. More than 90 genes coding potassium channel pore forming subunits have been identified, so far [3, 4]. Typical voltage-gated K^+ channels (Kv), mainly localized in axon nodes, between the axonal segments enwrapped by myelin sheaths, have a major role in generation and propagation of action potential, synaptic transmission, and regulation of the hormone secretion [5]. Astrocytes, as the most abundant cells in CNS, contribute to the physical and metabolic support to the neurons [6], including ion homeostasis [7]. The major role of Kv channels in astrocytes is removing a considerable excess of extracellular K^+, released from neurons during action potentials

✉ I. Lavrnja
irenam@ibiss.bg.ac.rs

[1] Department of Neurobiology, Institute for Biological Research "Siniša Stanković"- National Institute of Republic of Serbia, University of Belgrade, Belgrade, Serbia

[2] Department for General Physiology and Biophysics, Faculty of Biology, University of Belgrade, Belgrade, Serbia

[8, 9]. Thus, astrocytes play a regulatory role in K^+ clearance due to neuronal excitability [7, 8].

Since potassium channels are involved in important biological functions, including ion and water homeostasis and acid/base balance, it was suggested that potassium channelopathy may be the underlying cause or associated phenomenon in certain neurological diseases including MS/EAE [5, 10]. Indeed, potassium channels dysfunction has been observed in MS/EAE [11], in which a non-specific potassium channels blocker, 4-aminopyridine, induces beneficial effects on neurological function in chronic disease [12] and ameliorates the severity of the symptoms in relapsing–remitting form of EAE [13]. These findings suggest that 4-aminopyridine, already used as anti-symptomatic drug in the chronic phase of MS, can be used as a disease-modifying agent [14].

Another study shows that the use of a specific Kv1.3 channel blocker also ameliorates clinical symptoms in MS/EAE, by decreasing the number of activated T cells [15], supporting the stability of BBB [16] and inhibiting the inflammatory response of astrocytes [17]. It was additionally established that the Kv1.3 channel blocker preserves neuronal functionality and viability by preventing the respiratory burst in activated microglia [18]. Thus, the Kv1.3 channel proved to be a potential pharmacological target in MS/EAE. Studies have shown that Kv1.3 generates hetero-tetrameric complexes with Kv1.5 subunits [19], wherein the exact content of the channel complex determines the pharmacological and biophysical properties of the channel [20, 21].

Kv1.5 channel is a "*Shaker*-like" K^+ channel encoded by the *Kcna*5 gene. It was first cloned from rat heart tissue [22], but it is also found in pancreatic cells [23], pulmonary arteries [24], and skeletal and smooth muscles [25]. The expression of Kv1.5 in the brain is low [26], where its localization is limited to non-neuronal [27] and immune cells [28]. In the antigen-presenting cells, such as dendritic cells [29] and macrophages [30, 31], Kv1.3 and Kv1.5 form a mature hetero-tetrameric complex, wherein the cell activation depends on Kv1.3 subunits [32]. On the other hand, Kv1.5 may affect proliferation and differentiation in Schwann cells [33, 34], B-cells [35], microglia [36] and astrocytes [37, 38]. Therefore, it is suggested that the Kv1.3 governs the immune response, while the Kv1.5 fine-tunes it [32].

We have recently shown that expression of Kv1.3 channel increases in activated microglia and astrocytes during EAE. It has been also shown that the expression of Kv1.3 and Kv1.5 in the same pathological condition may be inversely regulated [5, 30]. The present study aimed to examine the expression of Kv1.5 channel in the spinal cord over the course of EAE and its cellular allocation. Here, we describe the temporal pattern of the Kv1.5 gene and protein expression in the spinal cord of EAE animals. The results show significant down-regulation of the Kv1.5 channel, particularly at the peak of disease. Our results, together with the finding of others, support the notion that Kv1.3 and Kv1.5 may be potential immunosuppressive targets in MS [39].

Materials and Methods

Experimental Animals

Experiments were conducted using 2-month-old male rats of the Dark Agouti (DA) strain from the local colony. Animals were housed under standard conditions, with constant temperature and humidity, 12 h light/dark cycles, and free access to food and water. All procedures were approved by the Ethical Committee for the Use of Laboratory Animals of Institute for Biological Research "Sinisa Stankovic" (Belgrade, Serbia), in compliance with EEC Directive (2010/63/EU) on the protection of animals used for experimental and other scientific purposes.

Induction of EAE and Evaluation of Disease Severity

Animals were randomly divided into control and the EAE group. Animals in the EAE group were anesthetized using carbon dioxide (CO_2) inhalation [40] and given a subcutaneous injection of spinal cord tissue homogenate in the hind footpad. The emulsion was prepared by mixing equal volumes of spinal cord homogenate (50% w/v in saline) and complete Freund's adjuvant containing 0.5% mg/ml Mycobacterium tuberculosis (CFA; Sigma, St. Louis, MO, USA). Animals were weighed, examined and scored for neurological signs of EAE daily, for 28 days post-immunization (dpi). Disease severity was assessed according to standard EAE scale: 0—without symptoms; 1—atony of tail; 2—hind limb weakness; 3—hind limb paralysis; 4—tetraplegic; 5—moribund state or death. The average daily score and weight were calculated and plotted for every time point. The disease was acute and monophasic, with 100% incidence and recovery. The first signs of EAE were apparent at 8 dpi, which was denoted as disease onset (Eo). The symptoms peaked at 14 dpi (Ep), after which the animals slowly recovered and showed no signs of the disease at 28 dpi, designated as the end of disease (Ee). The animals were anesthetized with Zoletil®50 (Virbac, France; 30 mg/kg i.p.), perfused intracardially with cold, sterile saline and sacrificed at three-time points: Eo, Ep, and Ee. The same procedure was performed on the age-matched, intact control animals. Spinal cords were isolated, lumbar sections excised and processed for RNA extraction, preparation of proteins for western blot and immunostaining.

Quantitative Real-Time PCR Analysis

Lumbar sections of the spinal cord were stored at − 80 °C in RNA later® stabilization solution (Invitrogen, Carlsbad, CA, USA), in order to preserve RNA until all groups were collected. RNA was isolated with TRIzol reagent (Invitrogen, Carlsbad, CA, USA), according to the manufacturer's instructions. The RNA concentration was assessed spectrophotometrically by measuring absorbance at 260 nm, and the purity was determined by calculating the ratio of absorbance at 260 nm and 280 nm. An equal amount of RNA (1 µg) from each sample was reverse transcribed to cDNA with High Capacity cDNA RT-kit (Applied Biosystems, Carlsbad, CA, USA). The obtained samples of cDNA were diluted 10 times and then used for qRT PCR analysis. Amplifications were performed with SYBR Green PCR Master Mix (Applied Biosystems, Foster City, CA, USA). Sequences for designated primers were as follows: *Kcna5*, forward: CCTGTCCCCGTCATCGTCTC; reverse: ACCTTCCGT TGACCCCCTGT; *Gapdh*, forward: CAACTCCCTCAA GATTGTCAGCAA; reverse GGCATGGACTGTGGTCAT GA Invitrogen, Carlsbad, CA, USA). PCR reactions were performed in the QuantStudio™ 3 Real-Time PCR System (Applied Biosystems, Foster City, CA, USA). Relative gene expression for *Kcna5* was evaluated by comparing Ct values for KCNA5 to Ct values of *Gapdh* as an internal control ($2^{-\Delta Ct}$ method). Results are expressed as mRNA levels of *Kcna5/Gapdh* relative to the control group.

Western Blot

Isolated lumbar sections of the spinal cord were pooled (3 for each group) and tissue was homogenized in RIPA buffer (50 mMTris pH 7.5, 150 mMNaCl, 1% NP-40, 0.1% SDS, 10 mM EDTA, 10 mM EGTA, 0.5% Triton X-100) with protease inhibitors (Roche, Penzberg, Germany). Samples were kept on ice and sonicated two times for 5 s and then centrifuged at 18,400×*g* for 30 min, at 4 °C. Supernatants were collected and their protein concentration was assessed using Micro BCA Protein Assay Kit, following manufacturer's instructions (Thermo Fisher Scientific, Rockford, IL, USA).

Equal protein amounts (10 µg) were resolved on 7,5% polyacrylamide gels and then transferred to polyvinylidene fluoride membrane (Immobilon-P transfer membrane, Millipore, Darmstadt, Germany) for 1 h at 100 V. After blocking unspecific binding with 5% Blotto in Tris-buffered saline (20 mMTris, pH 7.6, 136 mMNaCl) with 0.05% Tween 20 (TBST) for 1 h at room temperature, the membranes were incubated with primary antibody (Table 1) overnight, at 4 °C. After triple washing in TBST the membranes were incubated with appropriate secondary antibody linked with horseradish peroxidase (HRP, Table 1) for 2 h at room temperature. Protein bands were visualized with SuperSignal™ West Femto Maximum Sensitivity Substrate (Thermo Fisher Scientific, Rockford, IL, USA) and developed onto a film (KODAK, Rochester, NY, USA). Signal was quantified by densitometric analysis in ImageQuant 5.2 software by normalizing optical density of the Kv1.5 signal to β-actin of the same lane and the results are expressed relative to the control group.

Tissue Preparation for Immunostaining

Isolated sections of lumbar spinal cord tissue were fixed in 4% paraformaldehyde in 0.1 M phosphate buffer (PBS), pH 7.4 overnight at 4 °C and then cryoprotected in sucrose solutions of increasing concentrations (10–30% in 0.1 M PBS, pH 7.4). The spinal cords were subsequently frozen in 2-methylbutane and stored at − 80 °C. Coronal sections that were 20 µm thick were serially cut on cryotome, mounted on glass slides and stored at − 20 °C until all groups were collected and used for immunostaining for light and fluorescence microscopy.

Table 1 List of primary and secondary antibodies used for western blot (WB) and immunohistochemistry for light microscopy (IHC) and fluorescence microscopy (IF)

Antigen	Source	Dilution	Company
Kv1.5	Rabbit	1:500 WB 1:200 IHC, IF	Alomone, APC-004
β-actin	Mouse	1:5000 WB	Sigma, A5316
GFAP	Mouse	1:500 IF	NIH NeuroMab, clone73-240
ED1	Mouse	1:100 IF	Abcam, ab31630
Iba1	Goat	1:400 IF	Abcam, ab5076
Vimentin	Mouse	1:200, IF	Dako, M0725
Anti-rabbit IgG-HRP	Donkey	1:20,000 WB	Santa Cruz, sc-2305
Anti-mouse IgG-HRP	Donkey	1:20,000 WB	Santa Cruz, sc-2314
Anti-rabbit Alexa Fluor 555	Donkey	1:250 IF	Invitrogen, A31572
Anti-mouse Alexa Fluor 488	Donkey	1:250 IF	Invitrogen, A21202
Anti-goat Alexa Fluor 488	Donkey	1:250 IF	Invitrogen, A11055

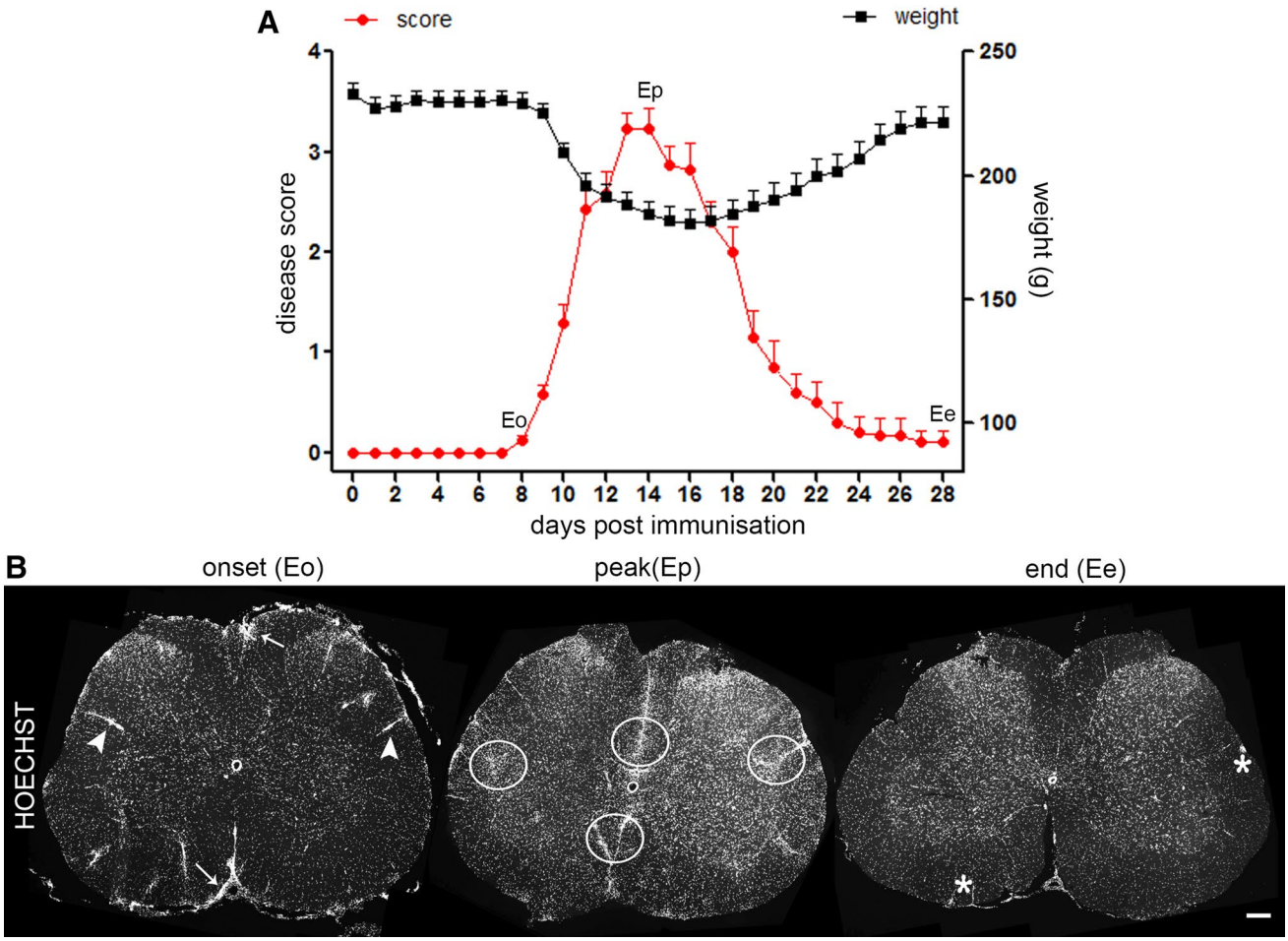

Fig. 1 Disease severity and CNS inflammation during the course of EAE. **a** EAE animals were followed over 28 days post-immunization (X-axis) and evaluated daily for body mass and neurological signs according to standard 0–5 grading scale as described in Materials and methods. The left Y-axis represents daily mean disease score ± SEM (red circles), while the right Y-axis represents daily mean body mass ± SEM (black squares). Three stages of EAE: onset (Eo), peak (Ep) and end (Ee) are indicated next to corresponding day post-immunization. **b** Since cellularity of spinal cord (SC) tissue is increased during EAE due to infiltration of peripheral immune cells, nuclear staining with Hoechst of lumbar SC cross-sections was used to follow the intensity of inflammation in three stages of the disease: Eo, Ep, and Ee. Infiltrating inflammatory cells are indicated with: white arrows (leptomeningeal area) and white arrowheads (CNS parenchyma) at Eo; white circle—widespread inflammation in CNS parenchyma at Ep; and white asterisks—remaining infiltrates at Ee. Scale bar: 200 µm (Color figure online)

Immunostaining for Light and Fluorescence Microscopy

Glass slides were incubated at room temperature for 30 min in order to acclimate the tissue before staining. The slides were washed in PBS and then endogenous peroxidase was blocked with 1% hydrogen peroxide in methanol. Next, the tissue was incubated in 0.1% Triton X-100 in PBS for 15 min to permeabilize cell membranes. After triple washing in PBS, the slides were incubated in 5% normal donkey serum for 1 h to block unspecific binding of antibodies. Subsequently, the tissue was incubated with the Kv1.5 channel antibody (Table 1) overnight, at 4 °C. On the next day, the slides were rinsed in PBS three times and incubated with HRP-conjugated donkey anti-rabbit antibody, for 2 h at room temperature. Kv1.5 was visualized with 3,3-S-diaminobenzidinetetrahydrochloride (DAB, Dako, Glostrup, Denmark). After dehydration in a sequence of alcohol solutions and xylene, the slides were mounted with DPX Mounting medium (Fluka, Buchs, Switzerland). The images were captured with the Leica DMRX 301-371.010 microscope (Leica Microsystems, Wetzlar, Germany), using × 10 magnification.

For immunofluorescent staining the protocol was similar, however blocking endogenous peroxidase was omitted. Specifications and dilutions for primary antibodies against cell-specific markers and appropriate fluorescently labeled secondary antibodies used in the study are given in Table 1. Nuclei were labeled with Hoechst 33342 dye (5 mg/ml,

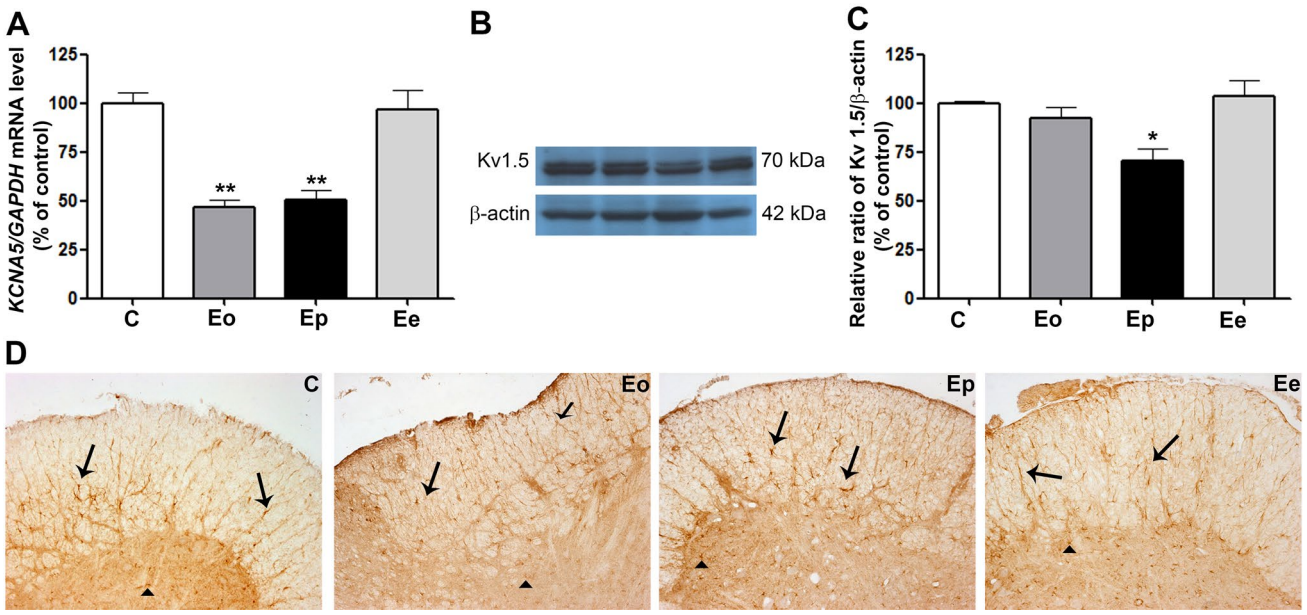

Fig. 2 Quantitative expression and visualization of Kv1.5 channel in the lumbar part of rat spinal cords during EAE. **a** *Kcna5* gene expression was assessed by qRT-PCR in immunized (Eo, Ep, and Ee) and naive animals (C—control), with GAPDH as an internal reference standard, and results expressed as mean % of control values ± SEM. **b** Protein levels of Kv1.5 were determined using the Western blot method, with β-actin used as a loading control, and **c** results expressed as mean % of control values ± SEM. $^{**}p < 0.001$ $^{*}p < 0.05$ compared to control. **d** Immunohistochemical visualization of Kv1.5 protein by DAB staining in lumbar SC cross-sections of control and EAE animals sacrificed at Eo, Ep, and Ee. Arrows and triangles are pointing to cells that morphologically resemble astrocytes in white and grey matter, respectively. Scale bar: 50 µm

Life Technologies, Invitrogen, Carlsbad, CA, USA) and this staining was also used to track inflammatory cells infiltration during EAE. The slides were mounted with Mowiol (Calbiochem, Millipore, Germany). Sections that were not incubated with the primary antibody solution showed no specific reaction. The images were captured with Zeiss Axiovert fluorescent microscope (Zeiss, Jena, Germany), using × 5 or × 63 magnifications and an Apotome system for obtaining optical sections.

Image Analysis and Quantification

Lumbosacral sections of the spinal cord labeled with Kv1.5/Iba1, Kv1.5/GFAP and Kv1.5/vimentin were used for quantification analysis to determine the expression of Kv1.5 on microglia and astrocytes, as described previously [17]. Briefly, sections from each group were divided into dorsal, ventral and left and right lateral segments of the white matter and three to five images of each segment were taken and examined with Image J software (National Institutes of Health, Bethesda, Maryland, USA). The images were analyzed for single labeled (Kv1.5, Iba1, GFAP, and vimentin) and double-labeled cells (Kv1.5/Iba1) or processes (Kv1.5/Iba1 and Kv1.5/vimentin) and compared to superimposed images. The results are expressed as the mean percentage of $Kv1.5^{+}$ cells of the total pool of $Iba1^{+}/GFAP^{+}/vimentin^{+}$ cells per group ± SEM.

Data Analysis

Statistical analysis was performed in GraphPad Prism 5 Software ® (GraphPad Software, La Jolla, CA, United States) using the Kruskal–Wallis test. Results are expressed as mean values ± standard error and values of $p < 0.05$ were considered to be statistically significant.

Results

Time Course of the EAE Pathology

All immunized animals developed the monophasic disease (Fig. 1a), with the onset (Eo) occurring typically around 8th day after immunization (8-dpi), peaking in severity at 14-dpi (Ep), and ending around 28-dpi (Ee). At the peak of the disease animals with severe neurological symptoms experienced significant body weight loss (Fig. 1a). The neurological scores obtained over the monophasic course of the illness are presented in Fig. 1b.

An autoimmune response initiated at the periphery by an injection of the encephalitogenic emulsion, caused a

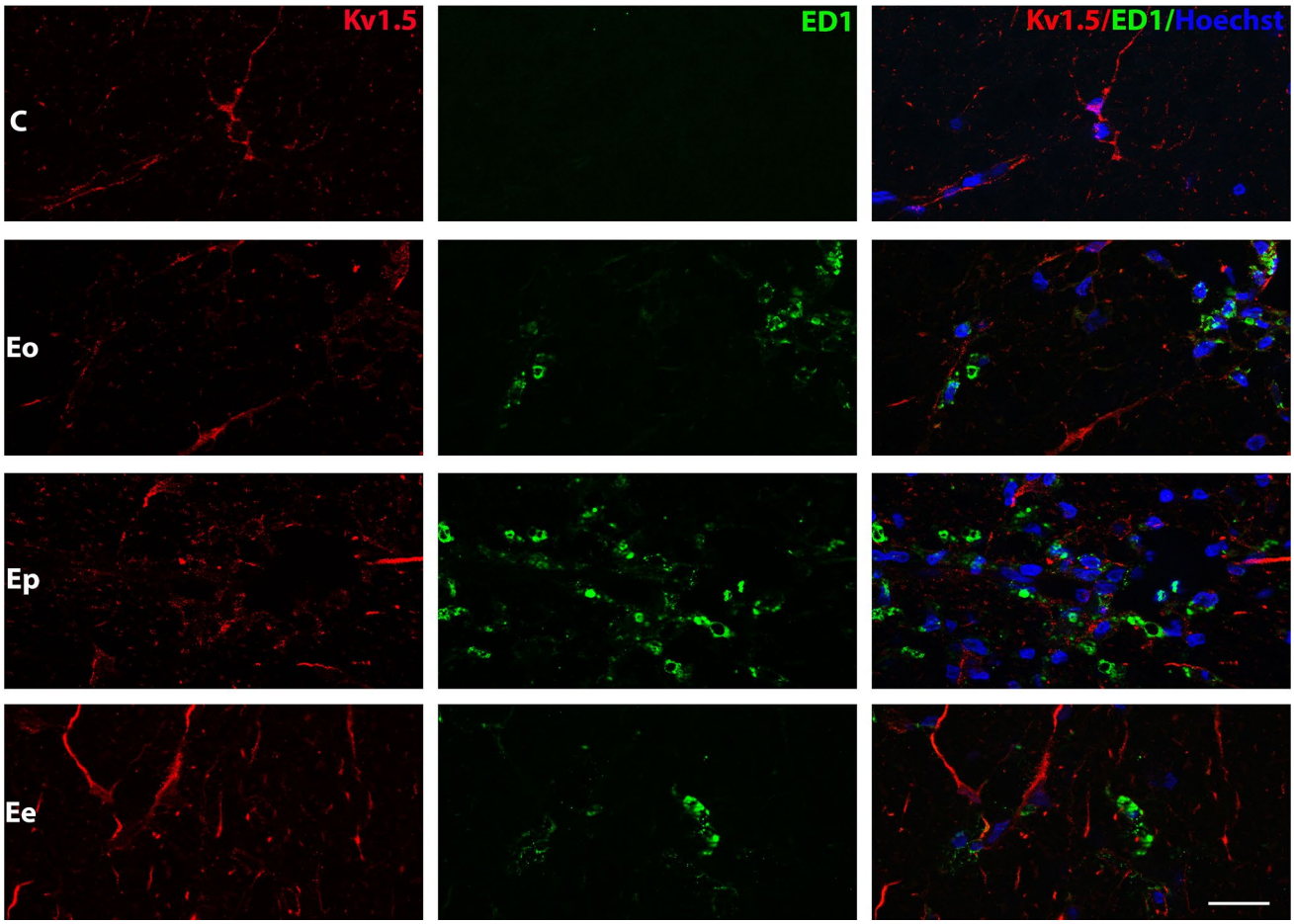

Fig. 3 Association of Kv1.5 with CNS myeloid cells in rat lumbar SC cross-sections. Kv1.5 (red fluorescence) was not found in ED1$^+$ cells (a marker of macrophages/microglia, green fluorescence), both in control and inflammatory conditions during EAE (Eo-onset, Ep—peak, Ee—end). Nuclear counterstain with Hoechst (blue). Scale bar: 20 µm (Color figure online)

neuroinflammatory reaction in the CNS, reflected in significant infiltration of peripheral immune cells into the spinal cord parenchyma and activation of astrocytes and microglia. Staining of nucleated cells in lumbar spinal cord sections of animals at different phases of EAE showed increased cellularity relative to healthy animals (not shown), due to the infiltration of inflammatory myeloid cells. The infiltrated cells at Eo were located close to leptomeninges (Fig. 1b, arrows) or in the perivascular zones along microvessels (Fig. 1 b, arrowheads). At the peak of disease, the infiltrates were more pronounced and widespread in the white matter parenchyma (Fig. 1b, circles). By the end of the disease, the mononuclear cells largely are withdrawn, leaving significantly smaller areas of infiltration (Fig. 1b, asterisks).

Expression of Kv1.5 Channel During EAE

Expression of Kv1.5 channel in the lumbar spinal cord over the course of EAE was assessed by qRT-PCR and Western blot (Fig. 2a–c). The abundance of Kv1.5-mRNA varied significantly during EAE, being about 50% less abundant at Eo and Ep relative to control, and returning to the baseline level at the end of disease (Fig. 2a). The abundance of the Kv1.5 protein, however, only slightly decreased at Ep, when about 25% reduction was observed relative to control (Fig. 2b, c). Immunohistochemisty labeling of Kv1.5 channel in the spinal cord tissue sections showed its wide distribution in control and EAE animals (Fig. 2d). The signal corresponding to the Kv1.5 channel mostly labeled cells that resemble fibrous (Fig. 2d, arrows) and protoplasmatic astrocytes (Fig. 2d, triangles).

Cellular Allocation of Kv1.5 Channel

Precise cellular allocation of Kv1.5 channel in the lumbar spinal cord was determined by double immunofluorescence labeling directed to Kv1.5 protein and cell-type specific markers.

The presence of Kv1.5 was determined in mononuclear phagocytes comprising resident microglia, and peripheral

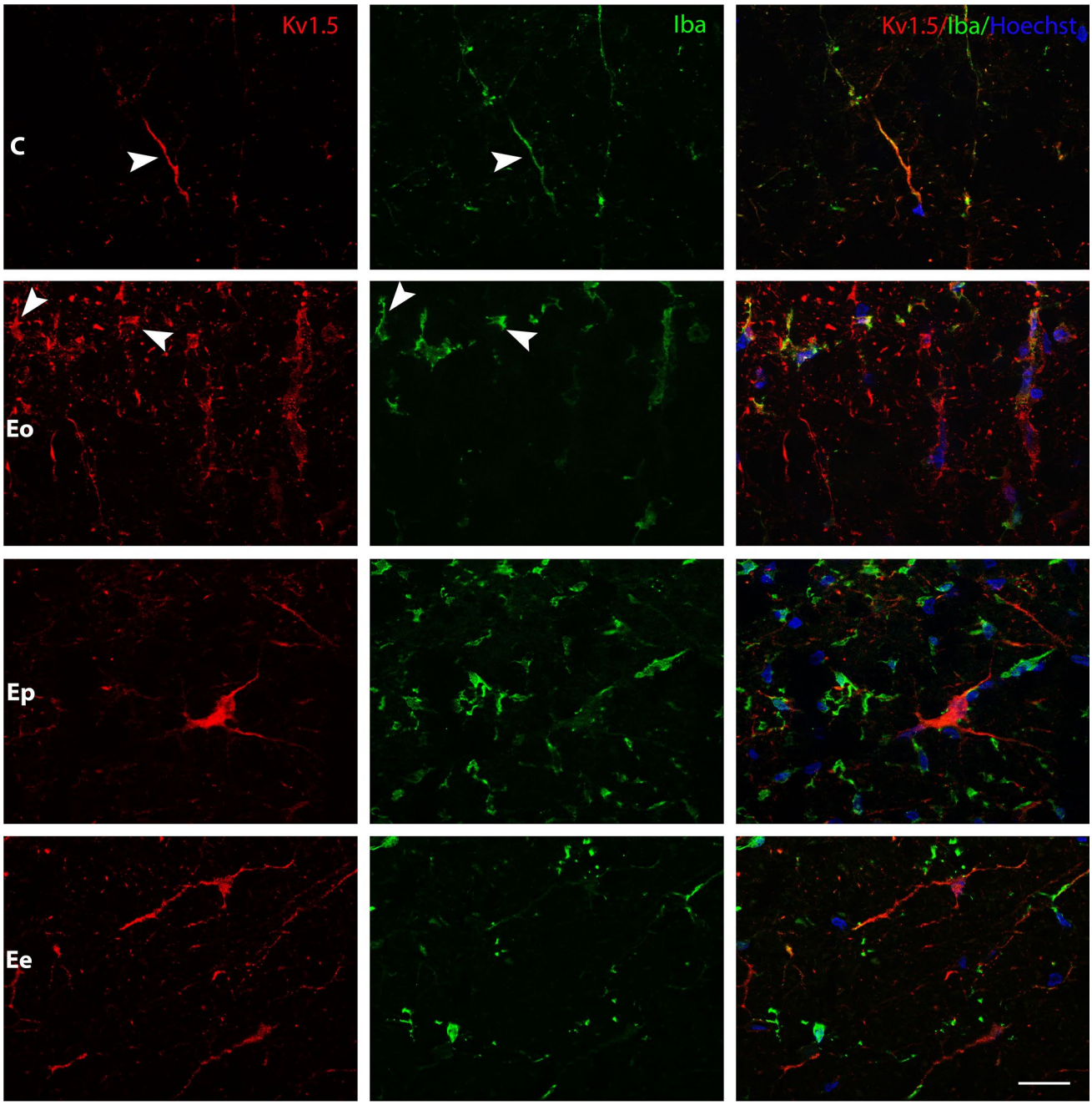

Fig. 4 Association of Kv1.5 with CNS resident immune cells—microglia, in rat lumbar SC cross-sections. Iba1 was used as a marker of microglia (green fluorescence). Kv1.5 (red fluorescence) was found in resting microglia of control animals and in $Iba1^+$ cells at the onset of EAE (Eo, arrowheads), while at peak (Ep) and the end (Ee) of EAE $Kv1.5^+Iba1^+$ cells were not found. Nuclear counterstain with Hoechst (blue). Scale bar: 20 µm (Color figure online)

macrophages that enter the spinal cord in pathological conditions. Both cell types are activated during EAE, with a culmination in their numbers at Ep (Figs. 3, 4, panel Ep). The identity of microglia/macrophages was established based on ED1 and Iba1 expression, wherein both markers being up-regulated upon the cell activation. The $ED1^+$ cells, which mostly populated the areas of cellular infiltration, did not appear to express Kv1.5 channel—at any phase of the disease (Fig. 3). Only sporadic co-expression of Kv1.5 and $Iba1^+$ were seen in cellular elements in control (Fig. 4, panel C—control animals, arrowheads; Fig. 7a), which most likely belong to resident microglia. Quantification of Kv1.5 expression on microglial cells showed that only 10% of the $Iba1^+$ cells in control sections expressed Kv1.5.

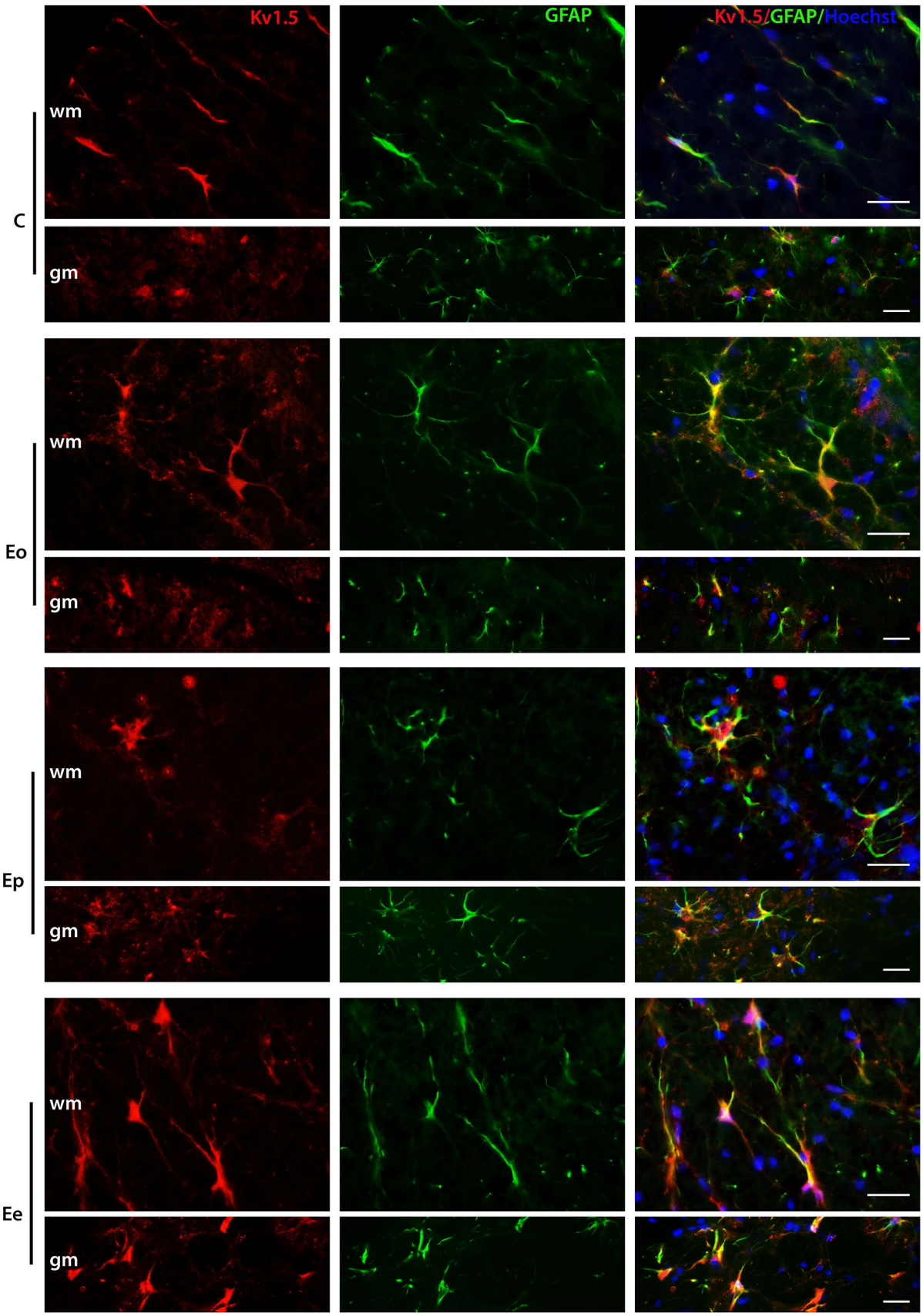
Kv1.5
GFAP
Kv1.5/GFAP/Hoechst
C
wm
gm
Eo
wm
gm
Ep
wm
gm
Ee
wm
gm

◂**Fig. 5** Association of Kv1.5 with GFAP$^+$ astrocytes, in rat lumbar SC cross-sections. Representative micrographs are showing that white and grey matter GFAP$^+$ astrocytes (green fluorescence) express Kv1.5 (red fluorescence), both in control and inflammatory conditions during EAE (Eo-onset, Ep—peak, Ee—end). Nuclear counterstain with Hoechst (blue). Scale bar: 20 µm (Color figure online)

After the onset of EAE, the percentage of Kv1.5$^+$ Iba1$^+$ cells decreased and at the end of disease these cells were not found (Fig. 7a). To summarize, the Kv1.5 channel does not appear to be significantly expressed by neither ED1$^+$ nor Iba1$^+$ cells during EAE.

Immunohistochemistry directed to Kv1.5 channel combined with light microscopy after DAB staining pointed to astrocytes as prevailing cells expressing Kv1.5 protein (Fig. 2d). Therefore, we next applied double immunofluorescence labeling directed to Kv1.5 channel and one of two astrocytes markers, GFAP for labeling mature astrocytes (Fig. 5) and vimentin for labeling proliferating immature astrocytes (Fig. 6). The immunofluorescence corresponding to Kv1.5 channel was found at GFAP$^+$ astrocytes regardless of the cell activation state, both in the white and grey matter over the course of EAE (Fig. 5), with around 60% of GFAP$^+$ astrocytes expressing Kv1.5 (Fig. 7b). At Ee, protoplasmic astrocytes expressed Kv1.5 channel most abundantly (Figs. 1d, 5, panel Ee; Fig. 7b). With regard to immature astrocytes, the cells positive to vimentin co-expressed Kv1.5 in all EAE phases (Fig. 6, arrows; Fig. 7c). At Eo and Ep, some vimentin$^+$/Kv1.5$^-$ cells were observed, probably round-shaped macrophages/microglia (Fig. 6, panel Eo, Ep, arrowheads). Taken together, our results suggest major allocation of Kv1.5 in fibrous and protoplasmatic GFAP$^+$ astrocytes over the course of EAE in addition to expression in vimentin$^+$ astrocytes in EAE rats.

Discussion

This study is the first to characterize spatiotemporal patterns of Kv1.5 expression at gene and protein levels, in the spinal cord over the course of EAE. We have shown that Kv1.5-mRNA abundance inversely correlates with disease severity and clinical scores. In addition, our study demonstrated that Kv1.5 protein is not expressed on infiltrating macrophages. Though it can be found scarcely on resting microglia in naïve rats, activated microglia cells are devoid of this channel during the disease course. Furthermore, GFAP$^+$ astrocytes express the Kv1.5 channel throughout the disease, while not all vimentin$^+$ astrocytes express this channel.

In our previous study, we have shown that the Kv1.3 channel gene and protein level increased at the peak of the disease, especially in activated macrophages/microglia and astrocytes [17]. It is well-known that besides Kv1.3, the Kv1.5 channel has a role in proliferation and activation processes in macrophages/microglia [20, 30, 31, 36]. During EAE, the proliferation and activation of macrophage/microglia increased at the peak of disease, as we have previously reported [41]. At this stage of activation, they are difficult to distinguish from recruited macrophages, however, it was suggested that the infiltrating macrophages are crucial for the EAE pathogenesis [42]. Macrophages act as principal inflammatory cells that are involved in MS/EAE disease progression and/or remission. Namely, macrophages, as antigen-presenting cells participate in governing immune response toward inflammation, including chemotaxis, myelin antigen presentation, secretion of several cytokines and chemokines and free radicals. On the other hand, macrophages are capable of phagocytosis of myelin proteins aiding the process of remyelination. In this study, immunohistochemistry analysis revealed that Kv1.5 protein was completely absent from ED1$^+$ macrophages/microglia cells at all stages of the disease. It was reported that the Kv1.5 channel is expressed on macrophages [30, 31], and during cell growth, a transition from Kv1.5 to Kv1.3 channel occurs [43]. Interestingly, we have shown previously that infiltrating macrophages/microglia express Kv1.3 during EAE [17]. In line with these findings, we can conclude that during EAE, Kv1.5 is not predominant channel presented on infiltrating macrophages/microglia, accordingly this channel does not have a role in macrophage activation. Although Kv1.3 is involved in the activation of macrophages [43], it was suggested that hybrid Kv1.3/Kv1.5 channel is predominant heterotetrameric channels in these cells [30], hence the Kv1.3/Kv1.5 ratio in myeloid cells might alter [31]. It was proposed that cytokines, such as TNF modify the stoichiometry of these subunits [30, 44]. Activated microglia secretes a number of pro-inflammatory cytokines, including TNF, whose increase is positively correlated to the EAE induction and progression of the disease [45, 46]. Khanna et al. demonstrated that Kv1.3 was present on the microglial cell membrane, whereas Kv1.5 was found mainly intracellularly [47]. In our previous study, we found that Kv 1.3 was absent from resting Iba1$^+$ microglia cells [17]. In this study, we showed that around 10% of ramified Iba1$^+$ microglial cells in naïve animals express the Kv1.5 channel. Kotecha et al. concluded that Kv1.3 channel is expressed in proliferating cells, while the Kv1.5 channel is found on non-proliferating cells [43]. The resting, ramified microglia are present in healthy animals, indicating that Kv1.5 is expressed mainly on non-proliferating cells that preserve healthy CNS homeostasis and plasticity [6]. Highly branched microglia, are the first myeloid cells that respond to any inflammation occurring in the CNS [7]. At the onset of the disease, occasional Iba1$^+$ branched cells expressing the Kv1.5 channel were observed. Previously, it was postulated that inflammation might increase the expression of Kv1.5 channels in microglia,

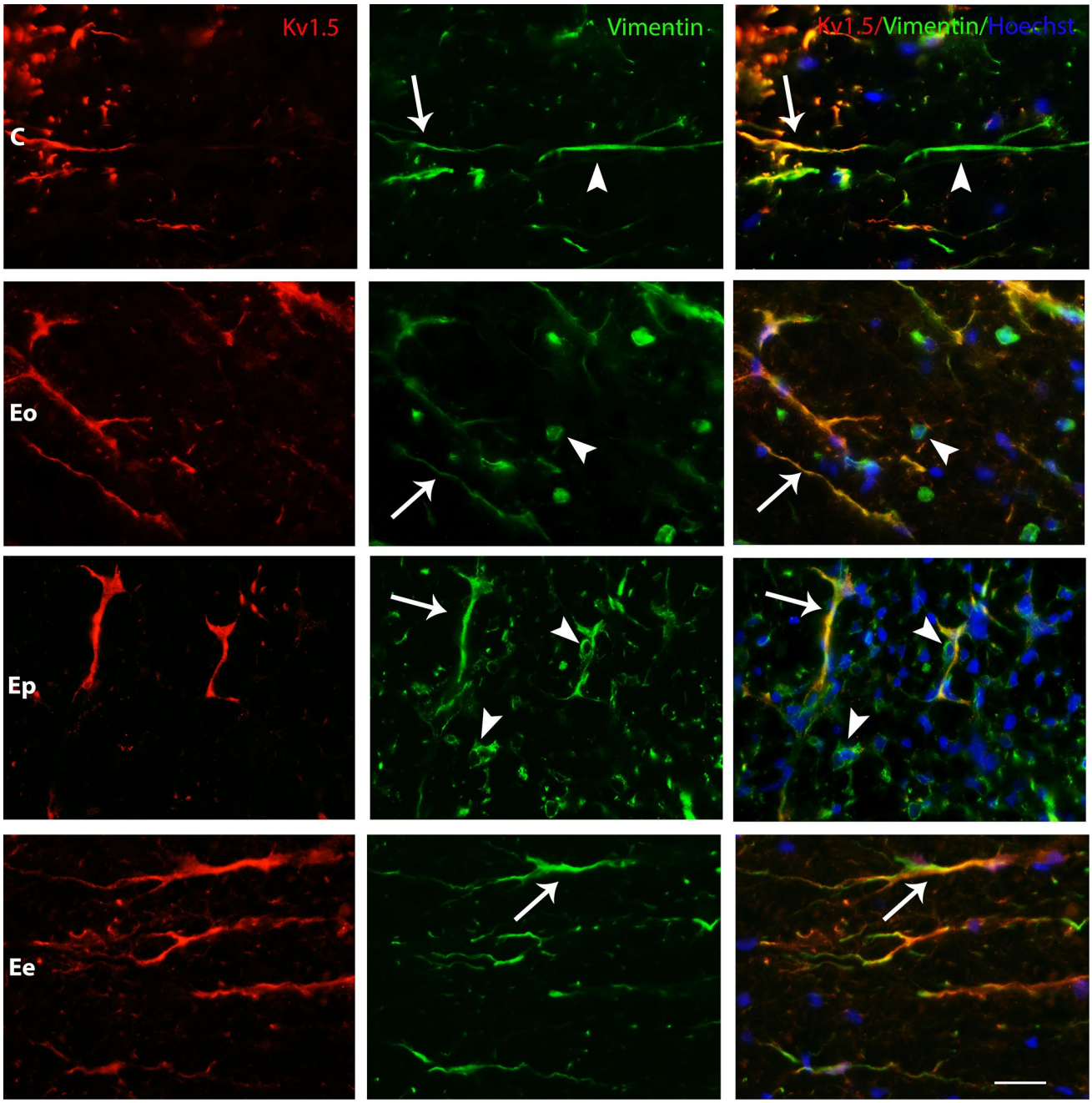

Fig. 6 Association of Kv1.5 with Vimentin$^+$ cells, in rat lumbar SC cross-sections. Double immunofluorescence labeling of Kv1.5 (red fluorescence) and vimentin (green) fluorescence with nuclear counterstain (Hoechst, blue). Vimentin$^+$Kv1.5$^+$astrocytes were found both in control and inflammatory conditions during EAE (Eo-onset, Ep—peak, Ee—end, arrows). Vimentin$^+$Kv1.5$^-$ cells that resemble: astrocytes were found in steady-state conditions (C—control, arrowhead); macrophages/microglia were found at the onset and peak of EAE (Eo and Ep, arrowheads). Scale bar: 20 µm

which is required for amplified NO production and inhibition of the cell cycle but not chemokine release [36]. This was in accordance with our previous study, where the highest iNOS level was observed at the onset of the disease [41]. It is interesting to note that during peak and recovery of EAE, Kv1.5 channel was completely absent from microglia cells, oppositely to Kv1.3 channels that show the specific expression on activated Iba1$^+$ microglia. Thus, the Kv1.3/Kv1.5 ratio may influence various physiological activities and can represent an indicator of cell activation [19, 30]. Specifically,

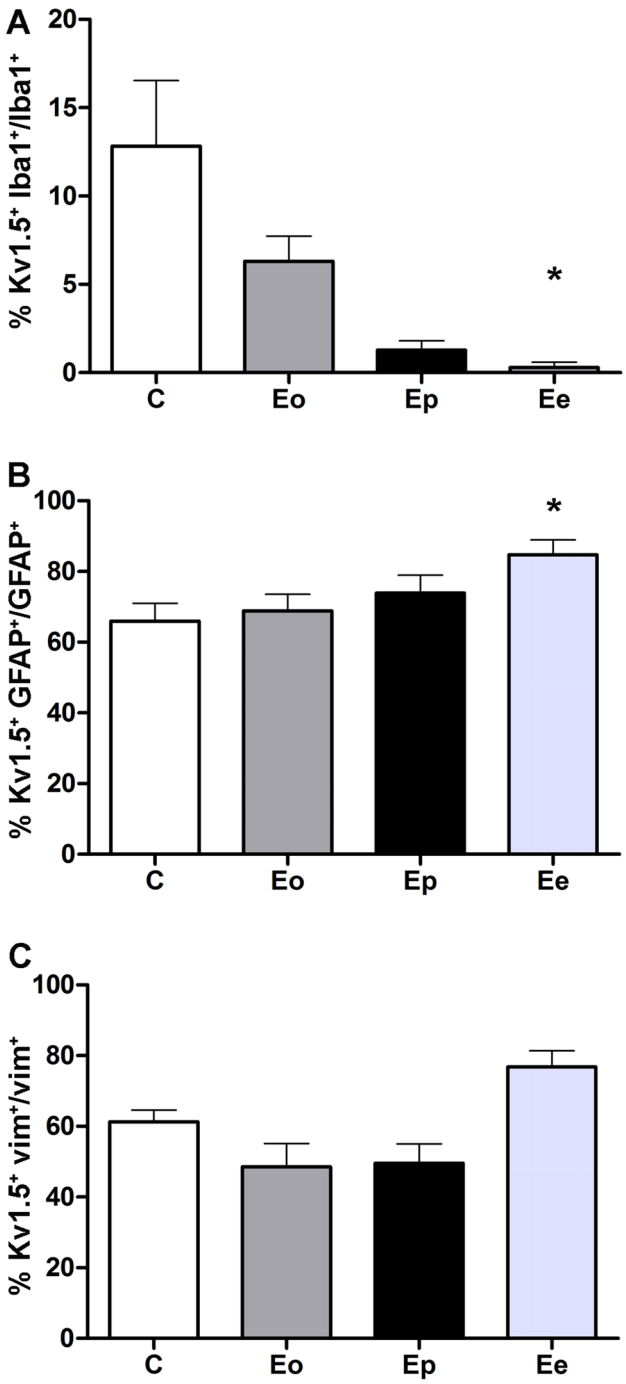

Fig. 7 Quantification of Kv1.5 expression on microglia and astrocytes in lumbar SC cross-sections. Changes in the percentage of Iba1$^+$ cells (**a**), GFAP$^+$ cells (**b**) and vimentin$^+$ cells (**c**) that express Kv1.5 in control animals and during EAE. Signifcance level inside the graph: *$p < 0.05$ compared to control

Kv1.3 channel expression is induced during activation and apoptosis, so its down-regulation is associated with immunosuppression [44], while high levels of Kv1.5 propose an immunosuppressive state of the cells [19, 21, 32]. Therefore, the amount of Kv1.3 and Kv1.5, with their complex can impact cell activation, proliferation, and/or differentiation [48]. Accordingly, modulation of macrophages/microglia activation was the basis for Kv1.3 blocker based therapy, so the link between Kv1.3 and Kv1.5 channels needs to be considered in designing Kv1.3 blocker-based therapy [31].

In the present study, we have shown that Kv1.5 channel expression largely coincided with GFAP$^+$ astrocytes in the white and grey matter of the rat spinal cord, while some vimentin + cells are devoid of Kv1.5 expression, mainly in naïve rats and at the onset and peak of disease. It is well established that astrocytes express Kv 1.5 channels in the brain and spinal cord [38]. In addition, its presence was confirmed in astrocytes cell culture and glioma cells [37, 49]. Although a specific function of this channel is unknown, it was postulated that the Kv1.5 channel has a role in the proliferation of astrocytes [37, 38]. The same study implies that astrocyte differentiation is not affected by Kv1.5 channel expression. Results obtained from this study show that the Kv1.5 channel is expressed in GFAP$^+$ fibrous astrocytes that reside in the white matter, and in star-shaped GFAP$^+$ protoplasmic astrocytes that occupy the gray matter during the disease, irrespectively of the stage of the disease [50, 51]. Another glial marker, vimentin, is the intermediate filament responsible for maintaining cell integrity [27]. It is expressed in immature astrocytes early in the development of the CNS and replaced with GFAP during maturation [28]. Interestingly, an earlier study found that vimentin is expressed by activated macrophages [52]. In this study, at the onset and peak of disease, Kv1.5 channel expression was devoid of vimentin + cells that morphologically resemble macrophages. During MS/EAE, the upregulation of GFAP and vimentin has been shown to be the hallmark of reactive astrogliosis [53, 54]. It is well-known that astrocyte heterogeneity in terms of morphology and physiology may influence the glial propensity to respond differently to inflammatory stimuli and affect the disease outcome [55]. In specific, reactive astrogliosis may be detrimental to neuronal recovery, however, an astrocytic scar may restrict inflammation to CNS and possibly induce neuroprotection [56]. Kv1.5 channel expression was mainly localized in GFAP$^+$ astrocytes at the end of disease, implying that this channel is expressed on mature astrocytes. Previously, we demonstrated that these intermediate filaments are upregulated during the disease [45]. It is interesting to note, that naïve rats do not express Kv1.3 channel on GFAP$^+$ and vimentin$^+$ astrocytes [17], while we have suggested that during neuroinflammation, Kv1.3 channels has a proinflammatory role in astrocytes. Interestingly, the present study revealed the expression of the Kv1.5 channels on non-reactive and reactive astrocytes. Reactive astrocytes acquire hypertrophic morphology, which is indicative of tissue damage. Those astrocytes, with enlargement of the cell soma and reduced process density, are usually found near demyelinating lesions [57, 58], as we

previously demonstrated in peak and end of the disease [45]. Although the Kv1.5 channel is expressed on astrocytes that proliferate and differentiate during EAE, the Kv1.5 gene and protein level decrease at the onset and peak of the disease, implying that absence from microglia cells in part leads to a diminished level of this channel. In addition, these results indicate that the Kv1.5 channel might be in homomeric composition in astrocytes, although it cannot be omitted from the fact that astrocytes form Kv1.3 and Kv1.5 complex, as it was reported previously [38].

To summarize, the main goal of our study was to elucidate the spatio-temporal expression profile of the Kv1.5 channel during EAE. Our results reveal that the presence of this channel is not found in ED1 expressing macrophages/microglia, however, Kv1.5 channels were found on non-proliferating, resting $Iba1^+$ microglia. Predominant expression of the Kv1.5 channel was found in astrocytes during EAE. Having in mind the innate ability of astrocytes to protect neurons appears to be a promising therapeutic target [59], the results obtained from this study suggest a possible link between the Kv1.5 channel and the pathophysiological processes in the EAE. Further studies are desirable to reveal the signals that initiate the observed alterations in Kv1.5 expression and to be set in the EAE and other diseases with the neuroimmune component.

Funding The funding was provided by Ministry of Education, Science and Technological Development of the Republic of Serbia No. III41014.

Compliance with Ethical Standards

Conflict of interest The authors declare they have no conflict of interest.

References

1. Bjelobaba I, Savic D, Lavrnja I (2017) Multiple sclerosis and neuroinflammation: the overview of current and prospective therapies. Curr Pharm Des 23(5):693–730
2. Jukkola PI, Lovett-Racke AE, Zamvil SS, Gu C (2012) K+ channel alterations in the progression of experimental autoimmune encephalomyelitis. Neurobiol Dis 47(2):280–293
3. Yost Spencer C (1999) Potassium channels: basic aspects, functional roles, and medical significance. Anesthesiology 90(4):1186–1203
4. Tian C, Zhu R, Zhu L, Qiu T, Cao Z, Kang T (2014) Potassium channels: structures, diseases, and modulators. Chem Biol Drug Des 83(1):1–26
5. Judge SIV, Bever CT (2006) Potassium channel blockers in multiple sclerosis: neuronal Kv channels and effects of symptomatic treatment. Pharmacol Ther 111(1):224–259
6. Sofroniew MV, Vinters HV (2010) Astrocytes: biology and pathology. Acta Neuropathol 119(1):7–35
7. Belanger M, Magistretti PJ (2009) The role of astroglia in neuroprotection. Dialogues Clin Neurosci 11(3):281–295
8. Bellot-Saez A, Kekesi O, Morley JW, Buskila Y (2017) Astrocytic modulation of neuronal excitability through K(+) spatial buffering. Neurosci Biobehav Rev 77:87–97
9. Seifert G, Henneberger C, Steinhauser C (2018) Diversity of astrocyte potassium channels: an update. Brain Res Bull 136:26–36
10. Wulff H, Castle NA, Pardo LA (2009) Voltage-gated potassium channels as therapeutic targets. Nat Rev Drug Discov 8(12):982–1001
11. Schattling B, Eggert B, Friese MA (2014) Acquired channelopathies as contributors to development and progression of multiple sclerosis. Exp Neurol 262:28–36
12. Gobel K, Wedell JH, Herrmann AM, Wachsmuth L, Pankratz S, Bittner S et al (2013) 4-Aminopyridine ameliorates mobility but not disease course in an animal model of multiple sclerosis. Exp Neurol 248:62–71
13. Moriguchi K, Miyamoto K, Fukumoto Y, Kusunoki S (2018) 4-Aminopyridine ameliorates relapsing remitting experimental autoimmune encephalomyelitis in SJL/J mice. J Neuroimmunol 323:131–135
14. Goodman AD, Brown TR, Krupp LB, Schapiro RT, Schwid SR, Cohen R et al (2009) Sustained-release oral fampridine in multiple sclerosis: a randomised, double-blind, controlled trial. Lancet (London, England) 373(9665):732–738
15. Beeton C, Wulff H, Standifer NE, Azam P, Mullen KM, Pennington MW et al (2006) Kv1.3 channels are a therapeutic target for T cell-mediated autoimmune diseases. Proc Natl Acad Sci USA 103(46):17414–17419
16. Huang J, Han S, Sun Q, Zhao Y, Liu J, Yuan X et al (2017) Kv1.3 channel blocker (ImKTx88) maintains blood-brain barrier in experimental autoimmune encephalomyelitis. Cell Biosci 7:31
17. Bozic I, Tesovic K, Laketa D, Adzic M, Jakovljevic M, Bjelobaba I et al (2018) Voltage gated potassium channel Kv1.3 is upregulated on activated astrocytes in experimental autoimmune encephalomyelitis. Neurochem Res 43(5):1020–1034
18. Fordyce CB, Jagasia R, Zhu X, Schlichter LC (2005) Microglia Kv1.3 channels contribute to their ability to kill neurons. J Neurosci 25(31):7139–7149
19. Comes N, Bielanska J, Vallejo-Gracia A, Serrano-Albarras A, Marruecos L, Gomez D et al (2013) The voltage-dependent K(+) channels Kv1.3 and Kv1.5 in human cancer. Front Physiol 4:283
20. Vicente R, Escalada A, Coma M, Fuster G, Sanchez-Tillo E, Lopez-Iglesias C et al (2003) Differential voltage-dependent K+ channel responses during proliferation and activation in macrophages. J Biol Chem 278(47):46307–46320
21. Villalonga N, David M, Bielanska J, Vicente R, Comes N, Valenzuela C et al (2010) Immunomodulation of voltage-dependent K+ channels in macrophages: molecular and biophysical consequences. J Gen Physiol 135(2):135–147
22. Roberds SL, Tamkun MM (1991) Cloning and tissue-specific expression of five voltage-gated potassium channel cDNAs expressed in rat heart. Proc Natl Acad Sci USA 88(5):1798–1802
23. Yan L, Figueroa DJ, Austin CP, Liu Y, Bugianesi RM, Slaughter RS et al (2004) Expression of voltage-gated potassium channels in human and rhesus pancreatic islets. Diabetes 53(3):597–607
24. Davies AR, Kozlowski RZ (2001) Kv channel subunit expression in rat pulmonary arteries. Lung 179(3):147–161
25. Bielanska J, Hernandez-Losa J, Moline T, Somoza R, Ramon y Cajal S, Condom E et al (2012) Differential expression of Kv1.3 and Kv1.5 voltage-dependent K+ channels in human skeletal muscle sarcomas. Cancer Investig 30(3):203–208
26. Swanson R, Marshall J, Smith JS, Williams JB, Boyle MB, Folander K et al (1990) Cloning and expression of cDNA and

genomic clones encoding three delayed rectifier potassium channels in rat brain. Neuron 4(6):929–939
27. Bielanska J, Hernandez-Losa J, Moline T, Somoza R, Ramon YCS, Condom E et al (2010) Voltage-dependent potassium channels Kv1.3 and Kv1.5 in human fetus. Cell Physiol Biochem 26(2):219–226
28. Villalonga N, David M, Bielanska J, Gonzalez T, Parra D, Soler C et al (2010) Immunomodulatory effects of diclofenac in leukocytes through the targeting of Kv1.3 voltage-dependent potassium channels. Biochem Pharmacol 80(6):858–866
29. Tyan L, Sopjani M, Dermaku-Sopjani M, Schmid E, Yang W, Xuan NT et al (2010) Inhibition of voltage-gated K+ channels in dendritic cells by rapamycin. Am J Physiol Cell Physiol 299(6):C1379–C1385
30. Vicente R, Escalada A, Villalonga N, Texido L, Roura-Ferrer M, Martin-Satue M et al (2006) Association of Kv1.5 and Kv1.3 contributes to the major voltage-dependent K+ channel in macrophages. J Biol Chem 281(49):37675–37685
31. Villalonga N, Escalada A, Vicente R, Sanchez-Tillo E, Celada A, Solsona C et al (2007) Kv1.3/Kv1.5 heteromeric channels compromise pharmacological responses in macrophages. Biochem Biophys Res Commun 352(4):913–918
32. Felipe A, Soler C, Comes N (2010) Kv1.5 in the immune system: the good, the bad, or the ugly? Front Physiol 1:152
33. Sobko A, Peretz A, Attali B (1998) Constitutive activation of delayed-rectifier potassium channels by a src family tyrosine kinase in Schwann cells. EMBO J 17(16):4723–4734
34. Sobko A, Peretz A, Shirihai O, Etkin S, Cherepanova V, Dagan D et al (1998) Heteromultimeric delayed-rectifier K+ channels in schwann cells: developmental expression and role in cell proliferation. J Neurosci 18(24):10398–10408
35. Vallejo-Gracia A, Bielanska J, Hernandez-Losa J, Castellvi J, Ruiz-Marcellan MC, Ramon y Cajal S et al (2013) Emerging role for the voltage-dependent K+ channel Kv1.5 in B-lymphocyte physiology: expression associated with human lymphoma malignancy. J Leukocyte Biol 94(4):779–789
36. Pannasch U, Farber K, Nolte C, Blonski M, Yan Chiu S, Messing A et al (2006) The potassium channels Kv1.5 and Kv1.3 modulate distinct functions of microglia. Mol Cell Neurosci 33(4):401–411
37. MacFarlane SN, Sontheimer H (2000) Modulation of Kv1.5 currents by Src tyrosine phosphorylation: potential role in the differentiation of astrocytes. J Neurosci 20(14):5245–5253
38. Roy ML, Saal D, Perney T, Sontheimer H, Waxman SG, Kaczmarek LK (1996) Manipulation of the delayed rectifier Kv1.5 potassium channel in glial cells by antisense oligodeoxynucleotides. Glia 18(3):177–184
39. Arnold R, Huynh W, Kiernan MC, Krishnan AV (2015) Ion channel modulation as a therapeutic approach in multiple sclerosis. Curr Med Chem 22(38):4366–4378
40. Kohler I, Meier R, Busato A, Neiger-Aeschbacher G (1999) Is carbon dioxide (CO2) a useful short acting anaesthetic for small laboratory animals? Lab Anim 33(2):155–161
41. Jakovljevic M, Lavrnja I, Bozic I, Milosevic A, Bjelobaba I, Savic D et al (2019) Induction of NTPDase1/CD39 by reactive microglia and macrophages is associated with the functional state during EAE. Front Neurosci 13:410
42. Trifunovic D, Djedovic N, Lavrnja I, Wendrich KS, Paquet-Durand F, Miljkovic D (2015) Cell death of spinal cord ED1(+) cells in a rat model of multiple sclerosis. PeerJ 3:e1189
43. Kotecha SA, Schlichter LC (1999) A Kv1.5 to Kv1.3 switch in endogenous hippocampal microglia and a role in proliferation. J Neurosci 19(24):10680–10693
44. Lampert A, Muller MM, Berchtold S, Lang KS, Palmada M, Dobrovinskaya O et al (2003) Effect of dexamethasone on voltage-gated K+ channels in Jurkat T-lymphocytes. Pflugers Archiv 447(2):168–174
45. Lavrnja I, Savic D, Bjelobaba I, Dacic S, Bozic I, Parabucki A et al (2012) The effect of ribavirin on reactive astrogliosis in experimental autoimmune encephalomyelitis. J Pharmacol Sci 119(3):221–232
46. Lavrnja I, Stojkov D, Bjelobaba I, Pekovic S, Dacic S, Nedeljkovic N et al (2008) Ribavirin ameliorates experimental autoimmune encephalomyelitis in rats and modulates cytokine production. Int Immunopharmacol 8(9):1282–1290
47. Khanna R, Roy L, Zhu X, Schlichter LC (2001) K+ channels and the microglial respiratory burst. Am J Physiol Cell Physiol 280(4):C796–C806
48. Stebbing MJ, Cottee JM, Rana I (2015) The role of ion channels in microglial activation and proliferation—a complex interplay between ligand-gated ion channels, K(+) channels, and intracellular Ca(2). Front Immunol 6:497
49. Preussat K, Beetz C, Schrey M, Kraft R, Wolfl S, Kalff R et al (2003) Expression of voltage-gated potassium channels Kv1.3 and Kv1.5 in human gliomas. Neurosci Lett 346(1–2):33–36
50. Nair A, Frederick TJ, Miller SD (2008) Astrocytes in multiple sclerosis: a product of their environment. Cell Mol Life Sci 65(17):2702–2720
51. Correale J, Farez MF (2015) The role of astrocytes in multiple sclerosis progression. Front Neurol 6:180
52. Mor-Vaknin N, Punturieri A, Sitwala K, Markovitz DM (2003) Vimentin is secreted by activated macrophages. Nat Cell Biol 5(1):59–63
53. Pekny M, Pekna M (2004) Astrocyte intermediate filaments in CNS pathologies and regeneration. J Pathol 204(4):428–437
54. Pekny M, Pekna M, Messing A, Steinhauser C, Lee JM, Parpura V et al (2016) Astrocytes: a central element in neurological diseases. Acta Neuropathol 131(3):323–345
55. Colombo E, Farina C (2016) Astrocytes: key regulators of neuroinflammation. Trends Immunol 37(9):608–620
56. Sofroniew MV (2015) Astrocyte barriers to neurotoxic inflammation. Nat Rev Neurosci 16(5):249–263
57. Ponath G, Park C, Pitt D (2018) The role of astrocytes in multiple sclerosis. Front Immunol 9:217
58. Sofroniew MV, Vinters HV (2010) Astrocytes: biology and pathology. Acta Neuropathol 119(1):7–35
59. Liu B, Teschemacher AG, Kasparov S (2017) Neuroprotective potential of astroglia. J Neurosci Res 95(11):2126–2139